July 2008
SLAC-R-904

# Lepton Flavor Violation in $\tau$ and $B$ decays at *BABAR*

Elisa Manoni
*Universitá di Perugia and I.N.F.N. sezione di Perugia, via A. Pascoli,* 06123*, Perugia, Italy*
(on behalf of the *BABAR* Collaboration)

Abstract

This article summarizes the search for lepton flavor violating $\tau$ and $B$ decays, using data collected by the *BABAR* detector at the PEP-II asymmetric-energy $B$ factory.

Work supported in part by US Department of Energy contract DE-AC02-76SF00515

## 1 Introduction

In the Standard Model (SM) with massless neutrinos, the lepton number is conserved separately for each generation. In this framework, Lepton Flavor (LF) conservation differs from other conservation laws because is not associated with an underlying conserved current symmetry. As a consequence extension of the SM or New Physics (NP) scenarios often include LF violation, as is also suggested by the discovery of neutrino oscillations [1]. In a modest extension of the SM incorporating finite $\nu$ mass, the branching ratios (BRs) of decays with LF violation are many orders of magnitude below the experimental accessibility. On the other hand, NP models predict enhancements on the BRs within the current experimental reaches and observation of LF violating processes would be a clear signature of NP and would allow to constraint parameters of such models. As an example, in Table 1 the predictions for $BR(\tau \to \ell\gamma)$ and $BR(\tau \to \ell\ell\ell)$ within several beyond-SM scenarios are shown; hereafter $\ell$ refers to a muon or an electron.
Here we present the most recent results on LF violating $\tau$ and $B$ decays at the *BABAR* experiment: $\tau^- \to \ell^-\ell^+\ell^-$ and $\tau^\pm \to \ell^\pm\omega$, $B^0 \to e^\pm\mu^\mp$, $B^0 \to \ell^\pm\tau^\mp$, and $B^+ \to K^+\tau^\mp\mu^\pm$. The *BABAR* detector, described in details elsewhere [2], collects data at the PEP-II asymmetric-energy $e^+e^-$ collider that operates at a center of mass (CM) energy of 10.58 $GeV$. The cross section production for $e^+e^- \to \tau^+\tau^-$ is $\sigma_{\tau\tau} \simeq 0.9\ nb$, and is comparable with the $e^+e^- \to B\bar{B}$ cross section production ($\sigma_{B\bar{B}} \simeq 1.05\ nb$): almost as many $\tau$ pairs as $B$ pairs are produced. Moreover, event shape variables allow to distinguish the jet-like topology of $\tau^+\tau^-$ from the sphericity of $B\bar{B}$ events. As a consequence, $B$ factories represent an optimal framework for this kind of investigation due to the high statistics and the clean environment in which both $\tau^+\tau^-$ and $B\bar{B}$ pair can be produced and distinguished by each other and by other events.

## 2 $\tau$ decays

### 2.1 Analysis Method

The analysis discussed in this paper concerning $\tau$ decays follow a common strategy. One $\tau$ is reconstructed in SM decays containing 1 or 3 tracks ("1-prong" or "3-prongs" topology) and from 1 to 2 neutrinos. The 1-prong category includes: $\tau \to \ell\nu_\ell\nu_\tau, \pi\nu_\tau, \rho\nu_\tau$, while the 3-prongs embodies $\tau \to 3\pi n\pi^0\nu_\tau$: all these modes covers roughly 99% of $\tau$ decays. The other $\tau$ is reconstructed in LF violating final states. The event is divided in two hemisphere using the plane perpendicular to the thrust of the event. The sign of scalar product of the given track momentum with the thrust direction determines the hemisphere to which the track belongs to. The thrust is calculated using charged and neutral

Table 1: *Predictions for $BR(\tau \to \ell\gamma)$ and $BR(\tau \to \ell\ell\ell)$ decays within several beyond-SM scenarios.*

| model | $BR(\tau \to \ell\gamma)$ | $BR(\tau \to \ell\ell\ell)$ |
|---|---|---|
| SM + $\nu$ mixing [3] | $10^{-54} - 10^{-40}$ | $10^{-14}$ |
| SUSY Higgs [4] | $10^{-10}$ | $10^{-7}$ |
| SM + heavy Majorana $\nu_R$ [5] | $10^{-9}$ | $10^{-10}$ |
| Non-universal $Z'$ [6] | $10^{-9}$ | $10^{-8}$ |
| SUSY SO(10) [7] | $10^{-8}$ | $10^{-10}$ |
| mSUGRA+seesaw [8] | $10^{-7}$ | $10^{-9}$ |

candidates in the CM frame. The side in which a 1- or 3-prong(s) decay is reconstructed is called "tag" side, while the other is the "signal" side. In Fig. 1 a sketch of a $\tau\tau$ event in the CM frame is shown. In the tag side at least one $\nu$ is present and the missing energy should be non zero, while on the signal hemisphere all the $\tau$ decay products are reconstructed. This condition allow to request that the reconstructed invariant mass ($m_{rec}$) and the CM energy ($E^*_{rec}$) for the signal side candidates are consistent with the nominal $\tau$ mass ($m_\tau^{PDG}$) and with the beam energy in the CM frame ($\sqrt{s}/2$) respectively. For signal events, the distribution of the two following variables:

$$\begin{aligned} \Delta m &= m_{rec} - m_\tau^{PDG} \\ \Delta E &= E^*_{rec} - \sqrt{s}/2 \end{aligned} \tag{1}$$

should peak at zero, with non Gaussian tails due to initial and final state radiation. For $\tau^- \to \ell^-\ell^+\ell^-$ channel values of the resolutions in $\Delta E$ and $\Delta m$ are 10 $MeV$ and $20 - 30$ $MeV/c^2$ (depending on the $3\ell$ combination) respectively. The resolution on $\Delta m$ can be improved by replacing $m_{rec}$ with the beam-energy constrained mass $m_{EC}$, computed from a fit to the reconstructed $\tau$ candidate decay products in which the $\tau$ energy in the CM is fixed to $\sqrt{s}/2$. This method is adopted in the $\tau^\pm \to \ell^\pm\omega$ analysis where the resolution in $\Delta m_{EC}$ ($\Delta E$) is $6 - 7$ $MeV/c^2$ ($31 - 32$ $MeV$) for $\ell = \mu, e$ respectively. Tracks used in the $\tau$'s reconstruction should satisfy particle identification (PID) criteria and a cut on their minimum momentum is applied. The total charge of the events is required to be zero. Events with tracks from gamma-conversion are rejected. Cuts on the kinematic properties of the tag side, such as momentum of the prong track(s), module and direction of the missing momentum, are applied. The selection criteria are optimized by using fully simulated signal and background Monte Carlo (MC) samples. The signal MC is also used to determine the signal efficiency, whose typical values are between 2% and 12%. Back-

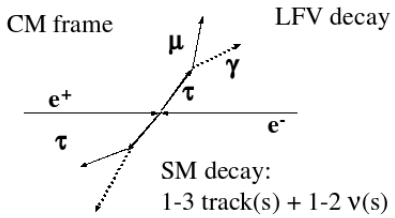


Figure 1: *Sketch of a $\tau\tau$ event in the CM frame: a SM decay in the tag side and a neutrinoless NP decay , i.e. $\tau \to \mu\gamma$, in the signal hemisphere are represented.*

ground MC and data and MC control samples are used to check the data-MC agreement and to model the background shapes of the relevant variables fitted with the purpose of estimating and subtracting the final background contribution. To avoid biases in the analysis a "blind" strategy is adopted: a signal region in the $\Delta E$-$m_{rec}$ (or $\Delta E$-$m_{EC}$) plane is defined around their central values with a width of $2-3$ standard deviations. The analysis procedure is tested outside the signal region (sideband); the same sample is also used for the background yield estimation, whose normalization is obtained from sideband data. Once the strategy is defined a 2-dimensional Maximum Likelihood (ML) fit is performed, the expected background yield and the fitted one are compared: if they are compatible, a 90% Confidence Level (CL) Upper Limit (UL) is set.

### 2.2 New *BABAR* results on $\tau^- \to \ell^-\ell^+\ell^-$ [10] and $\tau^\pm \to \ell^\pm\omega$ [11]

The $\tau^- \to \ell^-\ell^+\ell^-$ analysis has been performed on 376.0 $fb^{-1}$ corresponding to 346 million $\tau\tau$ pairs. All possible 3-lepton combinations, according to the charge conservation, are reconstructed. The signal signature consist of three charged tracks satisfying PID selection, whose invariant mass and energy are consistent with the $\tau$ hypothesis. For the tag side, the 1-prong topology is required. A 2 dimensional ML fit to the $m_{rec} - \Delta E$ distributions is performed. The search for $\tau \to (e,\mu)\omega$ has been performed on 384.1 $fb^{-1}$ (353 million $\tau^+\tau^-$ events). Signal decays are identified by a lepton track and a $(\pi^+\pi^-\pi^0)$ system in which the $\omega$ meson is reconstructed. The three charged tracks are fitted to a common vertex and the two photons from the $\pi^0$ are assumed to originate from the same point. Also a mass constraint on the $\pi^0$ is applied. The yield extraction is done by fitting the $\Delta E - m_{EC}$ distributions. A scatter plot of $\Delta E$ *vs* $m_{EC}$ after the selection is shown in Fig.2. The results of these

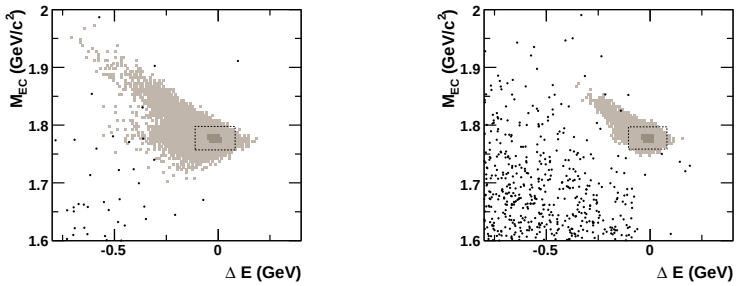


Figure 2: *Selected candidates (dots) in the $\Delta E - m_{EC}$ plane for $\tau^{\pm} \to e^{\pm}\omega$ (left) and $\tau^{\pm} \to \mu^{\pm}\omega$ (right). The signal box is shown by a dashed rectangle. The dark and light shading indicate contours containing 50% and 90% of the selected MC signal candidates respectively.*

two analysis are presented in Table 2.

### 2.3 Overview of measurements on $\tau$ decays and LF violation at *BABAR*

In Table 3 the results of the measurements performed by the *BABAR* collaboration on LF violation in $\tau$ decays are listed. A comparison with Belle is also reported. No evidence for signal is found in any of the channels under investigation, the experimental limits are going down to $10^{-8}$ and in some cases constraints on NP parameters can be set. $\tau$ physics will also be exploited in a future Super $B$ factory project, preliminary studies [9] have shown that improvements on the UL of factors $10-100$ with respect to the $B$ factories results can be achieved, with an integrated luminosity of 75 $ab^{-1}$.

## 3 $B$ decays

### 3.1 $B^0 \to e^{\pm}\mu^{\mp}$ [20]

$B^0 \to \ell^+\ell'^-$ decays (where $\ell^+\ell'^-$ stands for $e^+e^-$, $\mu^+\mu^-$, $e^{\pm}\mu^{\mp}$) happen thought a $b \to d$ transition with an internal quark annihilation and are helicity suppressed by a factor $(m_\ell/m_\tau)^2$. Such processes are sensitive to NP in a large set of Minimal Flavor Violation models [21]. In addition, $B^0 \to e^{\pm}\mu^{\mp}$ violates the LF conservation: while is predicted to have null BR within the SM, NP can enhance its decay rate up to $10^{-10} - 10^{-16}$ [22]. The analysis has been performed on a dataset of 347 $fb^{-1}$ ($384 \times 10^6 B\bar{B}$ pairs). Signal $B$ candidates are reconstructed by identifying two oppositely charged tracks originating from

Table 2: *Results for $\tau^- \to \ell^-\ell^+\ell^-$ and $\tau^\pm \to \ell^\pm\omega$ analysis: signal efficiency ($\epsilon$), number of expected background events ($Nb_{exp}$), number of observed events ($N_{obs}$), 90% CL UL on the BR ($UL(BR)$).*

| channel | $\epsilon(\%)$ | $Nb_{exp}$ | $N_{obs}$ | $UL(BR) \times 10^{-8}$ |
|---|---|---|---|---|
| $\tau^- \to e^-e^+e^-$ | $8.9 \pm 0.2$ | $1.33 \pm 0.25$ | 1 | 4.3 |
| $\tau^- \to \mu^-e^+e^-$ | $8.3 \pm 0.6$ | $0.89 \pm 0.27$ | 2 | 8.0 |
| $\tau^- \to \mu^+e^-e^-$ | $12.4 \pm 0.8$ | $0.30 \pm 0.55$ | 2 | 5.8 |
| $\tau^- \to e^+\mu^-\mu^-$ | $8.8 \pm 0.8$ | $0.54 \pm 0.21$ | 1 | 5.6 |
| $\tau^- \to e^-\mu^+\mu^-$ | $6.2 \pm 0.5$ | $0.81 \pm 0.31$ | 0 | 3.7 |
| $\tau^- \to \mu^-\mu^+\mu^-$ | $5.5 \pm 0.7$ | $0.33 \pm 0.19$ | 0 | 5.3 |
| $\tau^- \to e^-\omega$ | $2.96 \pm 0.13$ | $0.35 \pm 0.06$ | 0 | 11.0 |
| $\tau^- \to \mu^-\omega$ | $2.56 \pm 0.16$ | $0.73 \pm 0.03$ | 0 | 10.0 |

the same vertex. Two main variables are used to select good $B$ candidates:

$$m_{ES} = \sqrt{E^{*2}_{beam} - p^{*2}_B} \qquad (2)$$
$$\Delta E = E^*_B - \sqrt{s}/2$$

where the subscripts beam and $B$ refer to the $\Upsilon(4S)$ and $B$ candidate, while the asterisk denotes the $\Upsilon(4S)$ rest frame. For well reconstructed $B$, $m_{ES}$ ($\Delta E$) should be close to the $B$ meson mass ($0\ GeV$). A signal region in $m_{ES}$ and $\Delta E$ is defined. Contamination from $q\bar{q}$ is suppressed by cutting on event shape variables. The main $B\bar{B}$ background comes from $B^0 \to \pi\pi, \pi K$ decay in which there is lepton-hadron misidentification; this contamination is suppressed by applying PID requirements. QED background in which $e$ and $\mu$ come directly from $e^+e^-$ interaction is fighted by cutting on the minimum number of charged tracks in the event. To extract the signal yields for each $\ell\ell'$ combination a ML fit is performed: the variable used are $m_{ES}$, $\Delta E$ and a Fisher discriminant constructed by the momentum and the angle in the CM frame of each particle reconstructed in the event and not used in the signal side. The signal Probability Density Function (PDF) shapes are obtained form the MC sample while for the background control data sample are used. Table 4 summarizes the results of the analysis: no signal if found for any of the three $\ell\ell'$ combination and a 90% probability UL on the BR is set.

### 3.2 $B^0 \to \ell^\pm\tau^\mp$ [23]

$B^0 \to \ell^\pm\tau^\mp$ is potentially sensitive to NP effects due to contribution from neutral and charged non-SM Higgs mediated diagrams [4] [24]. In these frameworks

Table 3: *Overview of measurements on LF violating $\tau$ decays at BABAR and comparison with Belle: for each channel the 90% CL UL on the BR and the luminosity $\mathcal{L}$ are listed for both experiments. $h$ and $h^{'}$ to a $K$ or a $\pi$.*

| | *BABAR* | | Belle | |
|---|---|---|---|---|
| channel | $UL(BR) \times 10^{-8}$ | $\mathcal{L}$ $(fb^{-1})$ | $UL(BR) \times 10^{-8}$ | $\mathcal{L}$ $(fb^{-1})$ |
| $\tau \to e\gamma$ | 11.0 [12] | 232.2 | 12.0 [15] | 535.0 |
| $\tau \to \mu\gamma$ | 6.8 [12] | 232.2 | 4.5 [15] | 535.0 |
| $\tau \to \ell(\pi^0, \eta, \eta^{'})$ | $11.0 - 16.0$ [13] | 339.0 | $7.0 - 12.0$ [16] | 401.0 |
| $\tau \to \ell hh'$ | $7.0 - 48.0$ [14] | 221.4 | $20.0 - 160.0$ [17] | 158.0 |
| $\tau \to \ell\ell\ell$ | $3.7 - 8.0$ [10] | 376.0 | $2.0 - 4.1$ [18] | 535.0 |
| $\tau \to (e, \mu)\omega$ | $10.0 - 11.0$ [11] | 384.1 | $9.0 - 18.0$ [19] | 543.0 |

the BR for $B^0 \to \ell^{\pm}\tau^{\mp}$ is enhanced up to $2 \times 10^{-10}$. The search is performed on 342 $fb^{-1}$ ($378 \times 10^6 B\bar{B}$ pairs). The analysis technique consist on exclusively reconstructing one $B$ ($B_{tag}$) in specific hadronic mode and then searching in the rest of the event for the $\ell\tau$ signature that identify the signal B ($B_{sig}$). The hadronic channels are of the form $B \to D^{(*)}X$ where $X$ is a combination of up to nine kaons and pions. Cuts on $\Delta E$ and $m_{ES}$ of the reconstructed $B_{tag}$ are applied to check the consistency with a $B$ meson. The signal hemisphere should contain a high momentum electron or muon not belonging to the tag side. The second highest momentum track is assumed to be a $\tau$ daughter and should have opposite charge with respect to the primary signal lepton. Six $\tau$ decay modes are considered: $\tau \to e\nu_e\nu_\tau, \mu\nu_\mu\nu_\tau, \pi\nu_\tau, \pi\pi^0\nu_\tau, \pi 2\pi^0\nu_\tau, 3\pi\nu_\tau$. Once the electron or the muon is reconstructed, the $\tau$ kinematics is inferred by assuming the nominal energy and momentum of the $\tau$ for a 2-body $B^0$ decay. Background from non resonant $e^+e^- \to q\bar{q}$ decays is suppressed by exploiting event shape variables; contamination from beam background, unassociated hadronic shower fragments, reconstruction artifacts, bremsstrahlung, and photon conversion are reduced by cutting on the number of extra tracks and neutrals, the missing momentum and the extra energy. The latter describe the amount of energy recorded by the detector, not used in the $B_{tag}$ nor $B_{sig}$ reconstruction, while the missing momentum is associated to the undetected neutrinos. The signal yield is extracted by an unbinned ML fit to the distribution of the signal lepton momentum in the $B_{sig}$ rest frame (Fig.3); both signal and background PDF parametrization are determined from simulated events. The results of the analysis are presented in Table 4: these ULs represent the most stringent results on $B^0 \to (e, \mu)^{\pm}\tau^{\mp}$.

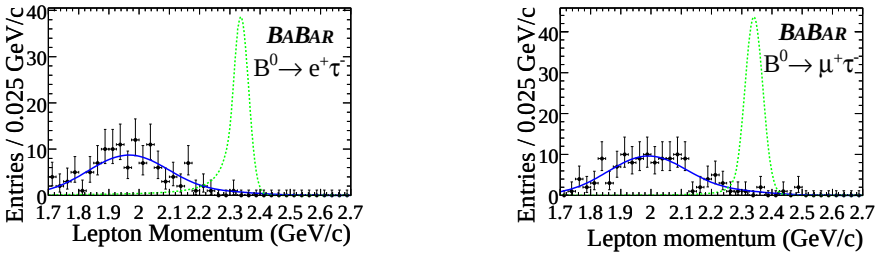


Figure 3: *The unbinned ML fits on the lepton momentum in the $B_{sig}$ rest frame (e-channel on the left, $\mu$-channel on the right), for $B^0 \to (e,\mu)^{\pm}\tau^{\mp}$ analysis. The dashed line represent the signal PDF with an arbitrary normalization, the solid line shows the background shape and the dots are the data.*

### 3.3 $B^+ \to K^+\tau^{\mp}\mu^{\pm}$ [25]

*BABAR* has recently published the first search for $B^+ \to K^+\tau^{\mp}\mu^{\pm}$. The process has higher sensitivity to NP with respect to $B^0 \to \ell^{\pm}\tau^{\mp}$, that is both helicity and CKM suppressed by a factor $|V_{td}/V^{cb}|^2$. In the frameworks of grand unified theories [26] with non-SM Higgs, the flavor changing neutral current Yukawa couplings between the $i^{th}$ and $j^{th}$ generations are proportional to $\sqrt{m_i m_j}/m_\tau$, leading to largest contributions in processes involving the second and third generation, as the $B^+ \to K^+\tau^{\mp}\mu^{\pm}$ do (both in the lepton and in the quark sector). A data sample of 347 $fb^{-1}$ ($383 \times 10^6 B\bar{B}$ pairs) has been used. The $B_{tag}$ meson if fully reconstructed in hadronic final states, while in the signal side a kaon candidate with opposite charge with respect to the $B_{tag}$, a muon and a third track with opposite charge with respect to the muon (identified as one of the $\tau$ daughter) are required. Only 1-prong $\tau$ decays ($\tau \to e\nu_e\nu_\tau, \mu\nu_\mu\nu_\tau, \pi\nu_\tau$) are considered, in order to reject combinatorial background. Having computed the $B_{sig}$ momentum in the CM frame as $-\vec{p}_{B_{tag}}$, the kinematics of the $\tau$ is completely inferred by $B_{sig}$, $K$ and $\mu$ momenta. PID criteria are required in the three tracks reconstruction. The main $B\bar{B}$ background contributions that survive the selection, are semileptonic $B$ decays with signature identical to the signal one, mainly $B^+ \to \bar{D}^0\mu^+\nu_\mu$ (where the $\bar{D}^0$ decays to $K^+\pi^-$ or to $K\ell\nu_\ell$ and the $\pi$ or the $\mu$ coming from the $D$ meson is identified as the $\tau$ daughter) and $B \to (c\bar{c})K$ decays (in which the $c\bar{c}$ resonance produce a muon pair). To reject this two contributions, cuts on the invariant masses of the kaon and the oppositely charged tracks and of the two non-kaon tracks are applied. The continuum background is suppressed using a likelihood ratio defined by event shape information, PID on the leptons and the signal

Table 4: *Results for* $B^0 \to \ell^+\ell'^-$ , $B^0 \to \ell^\pm\tau^\mp$, *and* $B^+ \to K^+\tau^\mp\mu^\pm$ *analysis: efficiency, number of signal events, 90% CL UL on the BR are listed. Note that* $\epsilon_{\ell\ell'}$ *and* $\epsilon_{K\tau\mu}$ *represent the signal efficiency while* $\epsilon$ *for the* $B^0 \to \ell^\pm\tau^\mp$ *incorporates also the tag efficiency.*

| | $B^0 \to \ell^+\ell'^-$ | | |
|---|---|---|---|
| channel | $\epsilon_{\ell\ell'}$ (%) | $N_{\ell\ell'}$ | $UL(BR) \times 10^{-8}$ |
| $B^0 \to e^+e^-$ | $16.6 \pm 0.3$ | $0.6 \pm 2.1$ | 11.3 |
| $B^0 \to \mu^+\mu^-$ | $15.7 \pm 0.2$ | $-4.9 \pm 1.4$ | 5.2 |
| $B^0 \to e^\pm\mu^\mp$ | $17.1 \pm 0.2$ | $1.1 \pm 1.8$ | 9.2 |
| | $B^0 \to \ell^\pm\tau^\mp$ | | |
| channel | $\epsilon(\times 10^5)$ | $N_{\ell\tau}$ | $UL(BR) \times 10^{-5}$ |
| $B^0 \to e^+\tau^-$ | $32 \pm 2$ | $0.02 \pm 0.01$ | 2.8 |
| $B^0 \to \mu^+\tau^-$ | $27 \pm 2$ | $0.01 \pm 0.01$ | 2.2 |
| | $B^+ \to K^+\tau^\mp\mu^\pm$ | | |
| $\tau$ channel | $\epsilon_{K\tau\mu}$(%) | $Nb_{exp}$ ; $N_{obs}$ | $UL(BR) \times 10^{-5}$ |
| electron | $3.28 \pm 0.25$ | $0.5 \pm 0.3$ ; 1 | |
| muon | $2.09 \pm 0.21$ | $0.6 \pm 0.3$ ; 0 | |
| pion | $2.18 \pm 0.26$ | $1.8 \pm 0.6$ ; 2 | |
| all | | | 7.7 |

side neutral energy. Signal yield is estimated by cutting and counting in the $m_\tau$ signal region ($[1.65, 1.90]$ $GeV/c^2$), the background is evaluated from the number of events outside this region (sideband) and the signal-to-sideband ratio obtained from background MC. The number of observed events in data is consistent with the background-only hypothesis and an upper limit on the BR of $7.7 \times 10^{-5}$ is set. The results are summarized in Table 4.

## 4 Conclusions

Observation of LF violation in $\tau$ and $B$ decays would be an unambiguous signature of NP, anyhow stringent UL can constraint NP parameters and disentangle between different scenario. In this article we have presented the latest results from *BABAR* . Two analysis on $\tau$ channel have recently been published: $\tau^- \to \ell^-\ell^+\ell^-$ and $\tau^\pm \to (e,\mu)^\pm\omega$. Many other neutrinoless $\tau$ transitions have been investigated: no evidence for signal has been found and ULs of the order of $10^{-8}$ have been set. Some of these analysis will be updated on the full *BABAR* dataset, and a consistent improvement can be achieved by a Super Flavor factory. On the $B$ sector three results have been

shown and the following UL have been set: BR($B^0 \to e^{\pm}\mu^{\mp}$)$< 9.2 \times 10^{-8}$, BR($B^0 \to (e,\mu)^+\tau^-$)$< (2.8, 2.2)\times 10^{-5}$, and BR($B^+ \to K^+\tau^{\mp}\mu^{\pm}$)$< 7.7\times 10^{-5}$. Preliminary studies show that a Super Flavor Factory can push the last two ULs down to $10^{-7}$ with a datasample of 75 $ab^{-1}$ [9].

## 5 Acknowledgments

The author wishes to thank the conference organizers for an enjoyable and well organize workshop. This work is supported by DOE and NSF (USA), NSERC (Canada), IHEP (China), CEA and CNRS-IN2P3 (France), BMBF and DFG (Germany), INFN (Italy), FOM (The Netherlands), NFR (Norway), MIST (Russia), MEC (Spain), and PPARC (United Kingdom).

## References

1. Y. Fukuda *et al* [Super-Kamiokand Collab.], Phys. Rev. Lett. **81**, 1562 (1998); Q.R. Ahmad *et al* [SNO Collab.], Phys. Rev. Lett. **89**, 011301 (2002); M.H. Ahn *et al* [K2K Collab.], Phys. Rev. Lett. **90**, 041801 (2003); K. Eguchi *et al* [KamLAND Collab.], Phys. Rev. Lett. **90**, 021802 (2003);.
2. B. Auber *et al* [*BABAR* Collab.], Nucl. Instrum. Methods Phys. Res. Sec. A **479**, 1 (2002)
3. B.W. Lee and R.E. Shrock, Phys. Rev. D **16**, 1444 (1997); T.C. Cheng and L. Li, Phys. Rev. Lett. **45**, 1908 (1980); X. Pham, Eur. Phys. J. **C8**, 513 (1999);
4. A. Dedes, J.R. Ellis, and M. Raidal, Phys. Lett. B **549**, 159 (2002); A. Brignole and A. Rossi, Phys. Lett. B **566**, 217 (2003);
5. G. Cvetic,C.O. Dib, C. Kim, and J. Kim, Phys. Rev. D **74**, 93011 (2006)
6. C. Yue,Y. Zhang,L. Liu Phys. Lett. B **547**, 252 (2002);
7. A. Masiero, S.K. Vempati, and O. Vives, AIP Conf. Proc. **805**, 99 (2006); T. Fukuyama, T. Kikuchi, and N. Okada, Phys. Rev. D **68**, 33012 (2003)
8. J.R. Ellis, J. Hisano, M. Raidal, and Y. Shimuzu Phys. Rev. D **66**, 115013 (2002)
9. M. Bona *et al*, hep-ex/07090451 (2007)
10. B. Aubert *et al* [*BABAR* Collab.], Phys. Rev. Lett. **99**, 251803 (2007)
11. B. Aubert *et al* [*BABAR* Collab.], Phys. Rev. Lett. **100**, 071802 (2008)

12. B. Aubert *et al* [*BABAR* Collab.], Phys. Rev. Lett. **96**, 041802 (2006)

13. B. Aubert *et al* [*BABAR* Collab.], Phys. Rev. Lett. **98**, 061803 (2007)

14. B. Aubert *et al* [*BABAR* Collab.], Phys. Rev. Lett. **95**, 191801 (2005)

15. B. Aubert *et al* [Belle Collab.], hep-ex/07050650

16. B. Aubert *et al* [Belle Collab.], Phys. Lett. B **648**, 341 (2007)

17. B. Aubert *et al* [Belle Collab.], Phys. Lett. B **640**, 138 (2006)

18. B. Aubert *et al* [Belle Collab.], Phys. Lett. B **660**, 154 (2008)

19. B. Aubert *et al* [Belle Collab.], hep-ex/07083276

20. B. Aubert *et al* [*BABAR* Collab.], Phys. Rev. D **77**, 032007 (2008)

21. A.J. Buras *et al*, Phys. Lett. B **500**, 161 (2001)

22. A.J. Buras, Acta Phys. Polon. B **34**, 5615 (2003); G. D'Ambrosio *et al*, Nucl. Phys. B **645**, 155 (2002)

23. B. Aubert *et al* [*BABAR* Collab.], hep-ex/08010697

24. W.S. Hou, Phys. Rev. D **48**, 2342 (1993)

25. B. Aubert *et al* [*BABAR* Collab.], Phys. Rev. Lett. **99**, 201801 (2007)

26. M. Sher and Y. Yuan, Phys. Rev. D **44**, 1461 (1991); T.P. Cheng and M. Sher, Phys. Rev. D **35**, 3484 (1987)